Crack Growth in Ferroelectric Ceramics Driven by Cyclic Polarization Switching

C. S. LYNCH,* L. CHEN, Z. SUO AND R. M. MCMEEKING
Department of Mechanical and Environmental Engineering, University of California, Santa Barbara, CA 93106

W. YANG
Department of Engineering Mechanics, Tsinghua University, Beijing, China

ABSTRACT: Ferroelectric ceramics are susceptible to stable crack growth under cyclic electric field of high magnitude. The stresses originate from mismatch strains induced by the electric field around inhomogeneities, such as processing flaws, terminated electrodes and the cracks themselves. The phenomenon is studied using a lead lanthanum zirconate-titanate ceramic. A flaw is indented on the surface of a ceramic sample. Subject to a cyclic electric field of magnitude exceeding the coercive field, cracks eminate from the flaw, in the direction perpendicular to the voltage drop. Tests relevant to the phenomenon are also performed. Polarization and strain as functions of applied electric field are measured at various temperatures and applied stresses. Discharge is demonstrated through an air gap between two ceramic plates subjected to a voltage drop. Models are presented that explain the cyclic nature of the crack growth.

INTRODUCTION

FERROELECTRIC ceramics have recently been used as large strain actuators. Such actuators rely on multilayer concepts, wherein electrodes alternate with ceramic layers. Each ceramic layer operates near the coercive field to deliver a large strain. Understanding of various degradation phenomena is essential to design devices and materials for better performance.

A class of phenomena involving electric field induced cracks has received attention recently. Experiments by Winzer et al. (1989), Uchino and Furuta (1992), and Cao et al. (1993) have shown that cracks grow in ferroelectric ceramics under cyclic electric field. The growth is stable, with the crack extending a finite amount on each cycle. The growth is appreciable only when the amplitude of the applied field is near or above the coercive field. Materials susceptible to such cracks are wide ranging; cracking has been observed in ferroelectrics, antiferroelectrics and relaxors. Cracks can grow at low loading frequencies, e.g., 1 Hz.

Existing theories assume that the medium inside a crack is either conducting (McMeeking, 1990; Suo, 1993), or insulating (McMeeking, 1989; Pak, 1990; Sosa and Pak, 1990; Suo et al. 1992). Terminated electrodes and cavities containing ionized gases are conductors. On the other hand, relative permittivities of ferroelectric ceramics exceed 10^3, so that gas-filled cavities and second phase inclusions are insulators with much smaller permittivity. Cracks intensify the electric field at the crack tip. An insulating crack intensifies a field applied perpendicular to the crack, but does not perturb a field parallel to the crack. Conversely, a conducting crack intensifies a field applied parallel to the crack, but not a field perpendicular to it. The crack driving force is different for the two types of crack, positive for a conducting crack and negative for an insulating crack.

Our experimental observations suggest that cracks may be subjected to conditions different from those assumed in the existing theories. First, the high electric field across the gap between the crack faces may cause electrical breakdown. Second, permittivity inhomogeneities caused by contact points along the crack face, with associated electric field concentrations, may cause local switching in the crack region prior to the overall sample, leading to a crack wedging mechanism. Third, heating in the crack region can cause large strain mismatches that contribute to the wedging mechanism. This paper presents experimental observations and preliminary mechanics models, using a lead lanthanum zirconate-titanate ceramic. The high field material properties pertinent to field concentrations around cracks are also examined.

MATERIAL CHARACTERIZATION

The material used in this study is a perovskite-type ceramic lead lanthanum zirconate-titanate $(Pb,La)(Zr,Ti)O_3$ (PLZT), of composition La/Zr/Ti = 8/65/35, with 5 μm grain diameter. The properties of the PLZT ceramics have been thoroughly investigated; see Haertling (1987) for review. Table 1 lists typical properties of two compositions

*Author to whom correspondence should be addressed.

1045-389X/95/02 0191-08 $10.00/0

Table 1. Properties of PLZT (Haertling, 1986).

Composition (La/Zr/Ti)	8/65/325	9.4/65/35
d_{33} ($\times 10^{-12}$ C/N)	682	0
P^R (C/m^2)	.30	0
E_c (MV/m)	3.6	0
T_c (°C)	110	25
25°C Phase	Ferro. Rh.	Slim Loop
ϵ_r	3350	5500
tan δ (%)	2.5	5.5
Resistivity (Ω-cm)	10^{13}	10^{13}
k	.648	0
S_{11} ($\times 10^{-12}$ m^2/N)	12.4	
Q_{11} (m^4/C^2)	.018	.021
Q_{12} (m^4/C^2)	−.008	−.009

of PLZT. The 8/65/35 composition is transparent in the unpoled and the slim loop states, translucent in the poled ferroelectric state, and birefringent under strain or electric field. In what follows we highlight material properties that are important to crack growth.

Effect of Temperature

Cyclic electric loading of a ferroelectric above its coercive field generates heat, as do electric field concentrations around flaws and repeated opening and closing of crack faces. At low frequencies, thermal conduction will result in a uniform temperature in the sample. At sufficiently high frequency, the temperature may be higher near the cracked region than in the bulk. This in turn would cause strain mismatches due both to local thermal expansion, and to the temperature dependence of the stress-strain-electric field constitutive relations.

To help quantify these effects, strain and polarization vs. electric field are measured at various temperatures. Our data are consistent with those previously published (e.g., Meng et al., 1985). The PLZT samples were cut to dimensions 2 × 3 × 20 mm^3 and polished to 1 μm diamond. Silver epoxy electrodes were placed on the long thin faces, and strain gauges bonded on a large face. Samples were connected to a Sawyer-Tower circuit with a 10 μF series capacitor, and immersed in a silicone oil bath with a K-type thermocouple. The oil was heated on a hot plate. The strain gauges were connected to a standard wheatstone bridge signal conditioner.

Figure 1 shows the measured longitudinal strain and electric displacement vs. the applied electric field (*S-E* and *D-E*) at various temperatures. The applied electric field cycles between ±1 MV/m. At 23.4°C the material is ferroelectric with broad hysteresis loops. As the temperature increases, the coercive field decreases. Above 75°C the material exhibits slim hysteresis loops. At higher temperatures, the electric displacement varies linearly with the applied electric field, and the strain varies quadratically with the electric field. Spans of strain and electric displacement decrease as the temperature rises.

An optical effect was also observed. At the low temperatures, the material transmits more light when the strain is driven to its most negative (compressive) value, and less light as the material switches and the strain is driven to more positive values. Consequently, the sample flashes as the polarization switches when viewed with transmitted light. As the material is heated the transmission increases until,

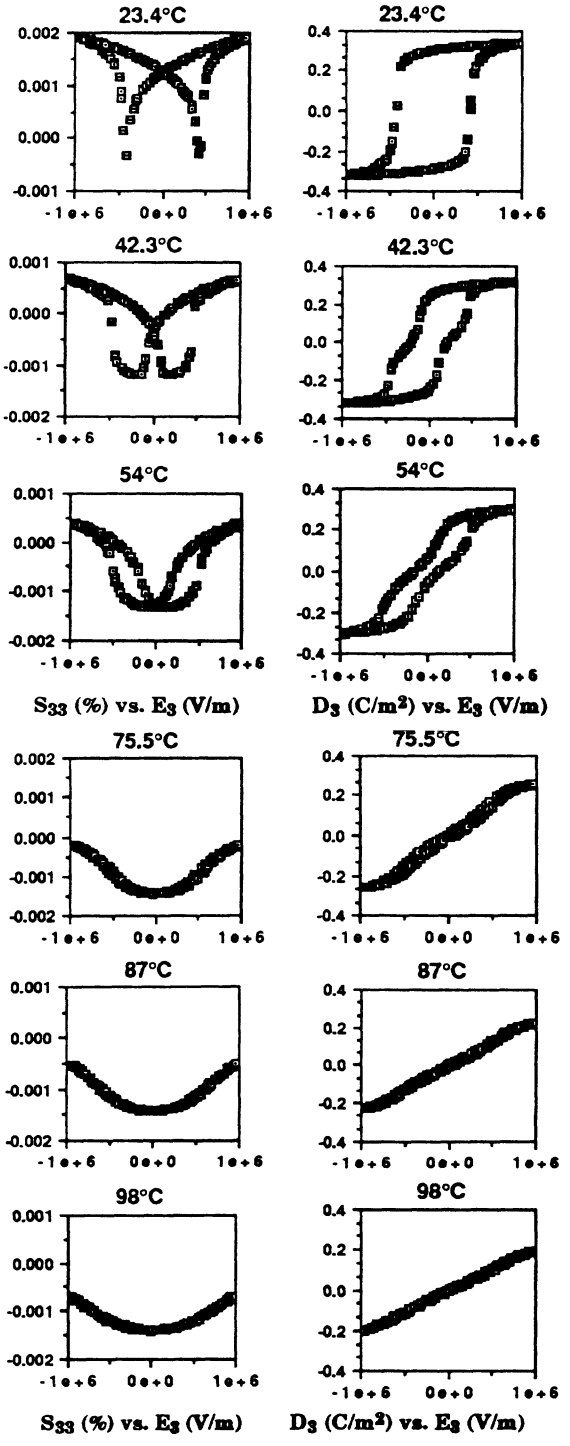

Figure 1. *Strain and electric displacement hysteresis loops for 8/65/35 PLZT at increasing temperatures.*

above 75°C, the material is transparent throughout the cycle.

Effect of Stress

Near a crack, large stresses develop which, in turn, affect the polarization switching. To quantify the effect of stress on switching, the *D-E* and *S-E* loops are measured as a function of uniaxial compressive stress applied parallel to the direction of polarization. The loading technique has been described elsewhere (Cao and Evans, 1993).

Figure 2 shows the effect of the uniaxial stress on the *D-E* and the *S-E* behavior at the room temperature. The uniaxial compressive stress strives to bring the material towards the state of lowest longitudinal strain. A small electric field also drives the material to a lower longitudinal strain and the effects are additive. As the electric field increases beyond the coercive field, the stress compresses the sample but the electric field extends it; the stress therefore hinders switching. At a compressive stress of 5 MPa the coercive field no longer makes a sharp transition, and switching is completed over a range of electric field. The hysteresis loops look similar to those at a slightly elevated temperature. At 10 MPa the switching spreads further and the residual strain at zero electric field is lower. This effect is even more pronounced at 50 MPa: the applied electric field is now almost unable to switch the material against the applied stress. At 90 MPa the hysteresis loops are substantially reduced.

A different type of experiment shows similar effects. With the sample connected to the Sawyer-Tower circuit and in the same mechanical loading fixture as above, the sample was first poled at zero stress. The stress was then monotonically increased to 90 MPa at zero electric field. The remanent polarization reduces from 0.3 C/m² to 0.18 C/m². The latter is consistent with the *D-E* loop under 90 MPa stress (Figure 2).

The *D-E* and *S-E* loops under stresses indicate the need to consider these effects when describing switching in the crack tip region associated with electric fatigue crack growth. Additional tests with the stress perpendicular to the electric field are needed to determine constitutive behaviors with coupled ferroelectric-ferroelastic switching at high fields.

DISCHARGE ACROSS A GAP BETWEEN TWO CERAMIC PLATES

The existing theories of field concentrations around cracks in dielectrics have assumed that the medium inside a crack is either conducting or insulating. These are the limiting cases. The large permittivity mismatch between the ceramic and the medium inside the crack (air or silicone oil) amplifies the electric field inside the crack. Such a high field may exceed the dielectric strength of the medium inside the crack, causing discharge between the two crack faces.

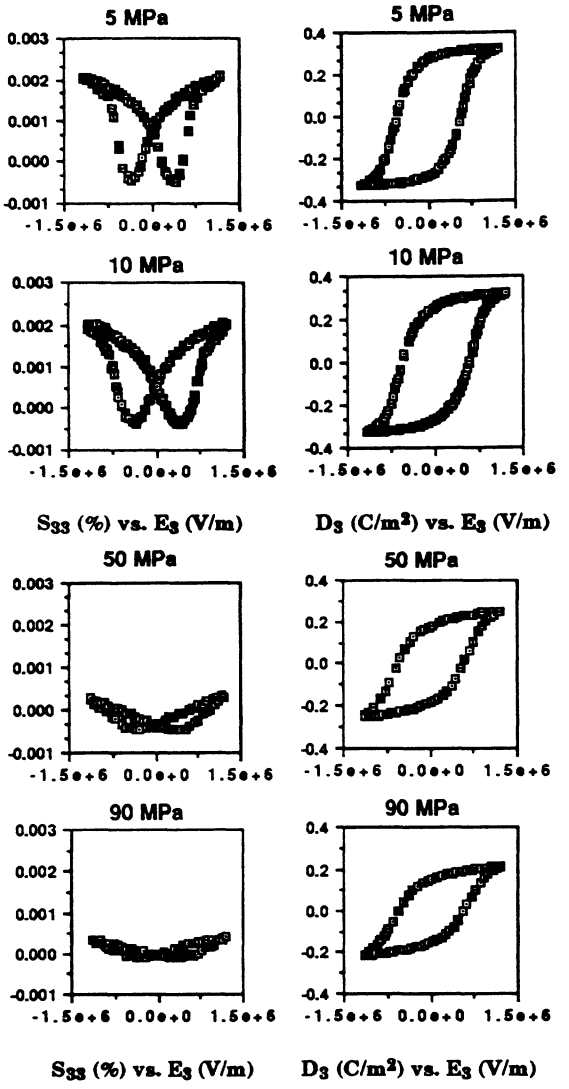

Figure 2. *Strain and electric displacement hysteresis loops for 8/65/35 PLZT at increasing uniaxial stress.*

The effect is examined experimentally with the setup illustrated in Figure 3. Two PLZT plates were cut 2.54 mm thick, ground, and polished to 1 μm diamond. The plates were bonded to two glass microscope slides with a thin film of silver epoxy. The silver epoxy extended beyond the sample and attached to a wire for electrical connection. The flat faces of the PLZT samples were placed together. A layer of quick set epoxy was placed on the surface of each glass slide opposite the samples and then placed between the grips of a test frame. The samples were pressed with a 20 N force to cure the epoxy. This step also held the faces parallel while fastening them to the test frame. The test frame was then transferred to displacement control with a resolution of ± 2 μm. The two halves were moved apart until the load cell read zero. The halves were then moved further apart to place a controlled size gap between the two plane surfaces.

The samples were connected to a Sawyer-Tower circuit and monotonically loaded with a variable DC power supply

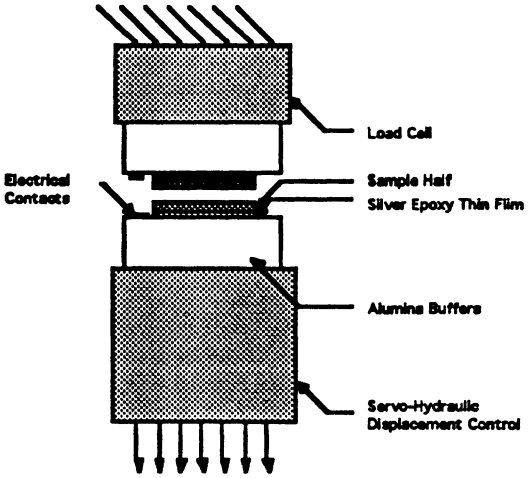

Figure 3. Experimental arrangement for the measurement of arcing across an air gap between two ferroelectric plates.

until arcing occurred. The results of the experiments are shown in Table 2. Blue sparks occurred in the gap as the material went through ferroelectric switching. At the first occurrence of sparks, the applied voltage was recorded. This was done for various gap sizes. When the sample was loaded above the coercive field then unloaded, the next cycle would only produce sparking if the loading was in the opposite direction. Reloading in the original direction gave no additional sparking. This indicated the charge was held on the surface by the remanent polarization. Next, the samples were cyclically loaded with a 50 μm gap and the *D-E* loop was recorded. As sparking occurred, noise appeared on the signal. This again indicated the arcing largely occurred during switching. To get a rough estimate of the breakdown field strength of the air gap we assume the entire voltage drop is across the gap; see the "Theoretical Considerations" section for justification. This corresponds to an infinite permeability. The calculated breakdown field is 70 MV/m for the 52 μm gap and 13 MV/m for the 200 μm gap.

CRACK GROWTH

Cao et al. (1993) reported the phenomenon of stable crack growth in PLZT under cyclic electric field. This section presents more detailed observations of such cracks. The effects of temperature, and the amplitude and frequency of the applied electric field are examined. Cracks are also independently produced by monotonic mechanical loading. The morphologies of the electrical and mechanical fracture surfaces are compared.

Cracking Driven by Cyclic Switching

PLZT samples are cut to dimensions 2 × 3 × 20 mm^3 and the four larger surfaces polished to 1 μm diamond. A Vicker's indenter is placed in the center of a 3 × 20 mm^2 surface with a 24.5 N load. This creates a square pyramid-shaped indentation of about 150 μm across a base diagonal with cracks emanating from the corners; the total flaw size including the microcracks is around 380 μm. Slow crack growth occurred over the following 24 hours. Silver epoxy electrodes are placed on the 2 × 20 mm^2 surfaces. The sample is connected to a Sawyer-Tower circuit, and observed through a microscope connected to a video camera. A scale is recorded to measure the crack length.

The fracture toughness of the PLZT is estimated by indentation data (Table 3). The method of Anstis et al. (1981) is used, namely

$$H = P/2a^2,\ K_{Ic} = 0.016(Y/H)^{1/2}(P/c^{3/2}) \qquad (1)$$

where H is the hardness, K_{Ic} the toughness, Y the Young's modulus, P the indent load, $2a$ diagonal of the indented pyramid base, and $2c$ the total crack length. Crack lengths were measured immediately after the indentation to avoid slow crack growth. In computing the hardness and the toughness, we have used P = 24.5 N and Y = 80.7 GPa.

Figure 4(a) shows an electrical fatigue crack in the early stages of growth near an indentation. The crack initially grows with branching. The general direction of growth is along the centerline of the sample perpendicular to the applied electric field. Figure 4(b) shows the crack tip region of the same crack after some growth. The crack appears as a dark shadow in transmitted light. When the specimen is viewed in reflected light or in the SEM, a single crack opening is observed [Figure 4(d)]. The surface chipping seen in

Table 2. Breakdown in air gap.

Gap Size (μm)	Voltage (KV)	Gap Size (μm)	Voltage (KV)
200	−2.8	600	−2.9
200	2.3	600	2.8
200	−2.6	600	−2.6
200	2.1	600	2.8
400	−2	52	2.7
400	1.4	52	−3.5
400	−1.5	52	
400	1.8	52	−3.5
400	−1.8	52	3.2

Table 3. Vicker's indentation data.

Test #	2a (μm)	2c (μm)	H (GPa)	K_{Ic} (MPa m$^{1/2}$)
1	200	370	1.23E+09	1.26
2	150	360	2.18E+09	0.99
3	150	360	2.18E+09	0.99
4	150	370	2.18E+09	0.95
5	150	400	2.18E+09	0.84
6	150	350	2.18E+09	1.03
7	150	380	2.18E+09	0.91

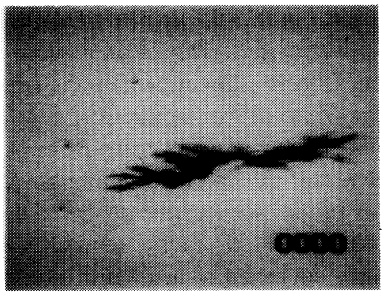

(a)

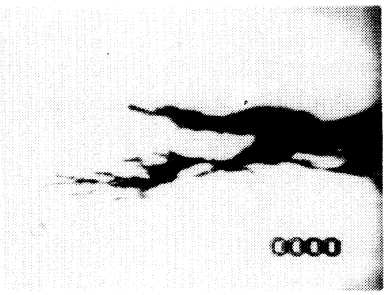

(b)

(c)

(d)

Figure 4. *Electric fatigue cracks in 8/65/35 PLZT: (a) transmitted light shows the early stage of crack growth around the Vicker's indent; (b) the growing crack; (c) scale (25.4 μm/DIV) for (a) and (b); (d) SEM shows the intersection of the crack with the surface. Crack growth vs. number of ferroelectric switching cycles at (e) 1.5 Hz; (f) 5 Hz.*

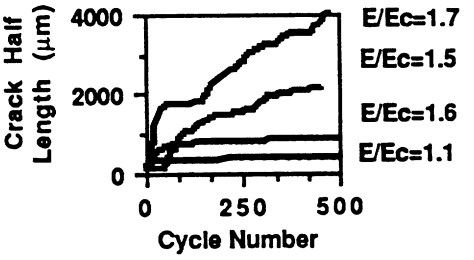

(e)

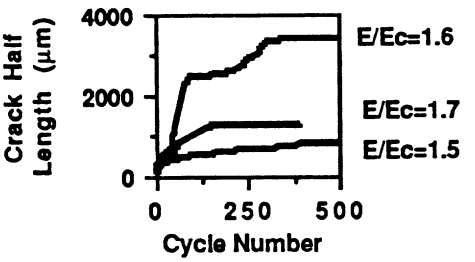

(f)

Figure 4 (continued). *Electric fatigue cracks in 8/65/35 PLZT: (a) transmitted light shows the early stage of crack growth around the Vicker's indent; (b) the growing crack; (c) scale (25.4 μm/DIV) for (a) and (b); (d) SEM shows the intersection of the crack with the surface. Crack growth vs. number of ferroelectric switching cycles at (e) 1.5 Hz; (f) 5 Hz.*

Figure 4(d) did not occur upon initial crack growth. The crack opens as the polarization switches, and closes as the polarization saturates. The chipping seems to indicate a mismatch in registration of the surfaces upon closure. This would be consistent with the development of wedging forces. The electric driven cracks run along grain boundaries. Figure 4(e) shows the dependence of crack growth rate on the applied electric field at 1.5 Hz. As the field strength is increased, the growth rate increases and there is less tendency for crack arrest. These samples were coated with silicone oil to prevent arcing between the electrodes and within the crack. Similar tests at 5 Hz [Figure 4(f)] indicate that growth rate is not a strong function of frequency.

Mechanical Cracks

Samples in the unpoled state were sliced to 150 μm thickness and polished to 1 μm diamond. The samples were placed on a microscope slide and Vicker's indented with a 2 N load. The thin samples buckled slightly and thus had a dominant crack across the center. The samples were attached to a test frame between crossed polarizers with quarter wave plates (standard photo stress setup), viewed with a microscope, and the results recorded on video tape.

Birefringence was observed around the indentation prior to mechanical loading. When the applied load was increased, a stress concentration became visible at the crack tips by a birefringence pattern [Figure 5(a)]. First the stress field grew, then stable propagation occurred followed by unstable failure. After failure, there was residual birefringence in the region of stable crack growth but none in

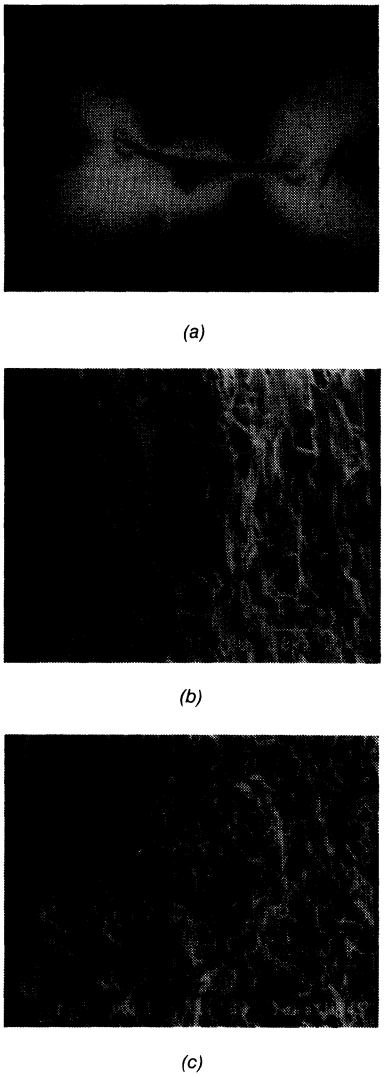

Figure 5. Mechanical crack in uniaxial tension: (a) birefringence shows stress field around Vicker's indentation in center and at crack tips (crack length 550 μm); (b) SEM displays transgranular crack growth near indentation site; (c) intergranular growth farther away.

the region of unstable growth. Figure 5(b) is a SEM micrograph of the fracture surface near the indentation. This region showed residual birefringence in the wake of the crack, and shows transgranular crack growth in the micrograph. Figure 5(c) is a SEM micrograph of a region away from the Vicker's indent. This region showed no residual birefringence and intergranular growth. The residual birefringence may be associated with ferroelastic switching in the wake of the crack.

THEORETICAL CONSIDERATIONS

Electric Field in Cavity or Gap

The electric field in a cavity within a dielectric is uniform. Since the tangential component of electric field is continuous, the crack tip field is equal to the internal field. The amplitude is equal to the applied field multiplied by the ratio of the permittivities. This is the largest possible field concentration. If there is arcing within the crack, a layer of surface charge will coat the fracture surfaces. There will no longer be a continuous normal component of electric displacement, and the electric field within the crack will be reduced. This in turn reduces the crack tip field.

First consider an elliptic cavity, semi-axes a and b, in a ceramic sample subjected to a uniform electric field E_{appl} along the b-axis remote from the cavity. The ceramic is assumed to be linearly dielectric with the dielectric constant $\varkappa > 10^3$. The medium inside the cavity is also dielectric with the dielectric constant close to unity. The field in the ceramic near the cavity is nonuniform, but the field inside the cavity E is uniform and directed along the b-axis. A classical result gives (Osborn, 1945)

$$\frac{E}{E_{appl}} = \frac{\varkappa + \varkappa b/a}{1 + \varkappa b/a} \tag{2}$$

Thus, for an equiaxed cavity ($b/a \approx 1$) in a high permittivity ceramic, the electric field inside the cavity is amplified by $E/E_{appl} \approx 2$. For a crack like cavity, the field inside the cavity can be much more amplified; in the limit $\varkappa b/a \ll 1$, $E/E_{appl} \to \varkappa$.

Next consider a gap between two ceramic plates. A voltage V drops over the total thickness of the two plates H, and the thickness δ of the air gap. The electric displacement is the same in the air and the ceramic, so that $E_{gap} = \varkappa E$. The electric field in the air gap is

$$E_{gap} = \varkappa \frac{V}{H} \frac{1}{1 + \varkappa\delta/H} \tag{3}$$

If the ceramic is loaded beyond the coercive field, say $E = 1$ MV/m, the field in the air gap exceeds $E_{gap} = 1$ GV/m. It is uncertain what the breakdown field of an air gap around $\delta = 1$ μm is, but a field of magnitude 1 GV/m exceeds the breakdown strength of most insulating thin films. Whether discharge happens is important in determining the electric field near the crack tip. This uncertainty needs to be resolved in future studies.

Wedging Induced by Localized Switching

This mechanism has been outlined by Cao et al. (1993). At the coercive field, the crack faces do not maintain a perfect registry: some patches are in contact but others remain open. The nonuniform permittivity distorts the electric field near the crack faces, as shown in Figure 6, so that the contact regions feel a higher field than the coercive field. Observe that the strain rises sharply when the electric field just exceeds the coercive field in a ferroelectric ceramic (Figure 1 room temperature). Consequently, the contact patches expand by a large strain $\tilde{\gamma}$, leading to a wedging mechanism.

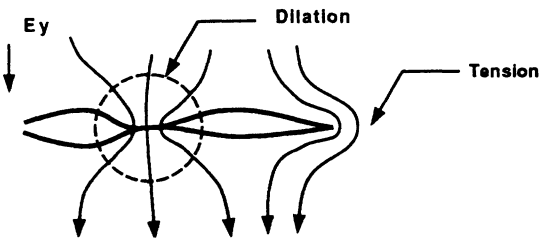

Figure 6. *Field concentration at contact points along crack faces.*

An estimate of the effect is given as follows. Denote the size of the contact patches to be λ. The additional displacement due to the localized switching is approximately given by

$$w \approx \lambda\tilde{\gamma} \tag{4}$$

This is equivalent to the wedge thickness. The stress intensity factor induced by the wedge is given by (Tada et al., 1985)

$$K = \frac{1}{\sqrt{8\pi}} \frac{wY}{\sqrt{\Delta a}} \tag{5}$$

where Δa is the crack extension per cycle. The crack extends if K reaches the fracture toughness of the ceramic, K_c. A combination of the two equations gives

$$\Delta a \approx \frac{1}{8\pi}\left(\frac{\lambda\tilde{\gamma}Y}{K_c}\right)^2 \tag{6}$$

Take $\lambda = 5$ μm (grain diameter), $\tilde{\gamma} = 3 \times 10^{-3}$, $Y = 100$ GPa, $K_c = 1$ MPa$\sqrt{\text{m}}$, one obtains $\Delta a = 0.1$ μm. This extension per cycle is smaller than that experimentally observed, but uncertainties in the estimate can substantially change the result.

If discharge has occurred during the previous loading cycle, the residual charge left after crack closure can also cause a localized electric field that induces switching in the crack region prior to the overall sample.

Global Strain Mismatch

A global strain mismatch is possible when the electric field in the overall sample exceeds the coercive field and the crack opens. Owing to the voltage drop across the crack faces, the electric field in the ceramic ahead of the crack is larger than the electric field behind the crack. This field difference causes the ceramic ahead the crack to expand more than that behind. As a crude approximation, we assume that the electric field is piece wise uniform, being E_1 behind and E_2 ahead the crack [Figure 7(a)]. The corresponding misfit strain is γ_M. The stress intensity induced by this global misfit can be calculated by a superposition (Eshelby's cut-and-paste). The strain would be matched if the two arms were stressed in tension by $\sigma = Y\gamma_M$, where Y is the elastic modulus [Figure 7(c)]. To eliminate the tensile stress, a compressive stress is added to the two arms [Figure 7(d)]. The stress intensity factor in Figure 7(d) is given by

$$K = Y\gamma_M\sqrt{H/2} \tag{7}$$

Take $Y = 100$ GPa, $H = 200$ μm and $\gamma_M = 10^{-4}$, one obtains that $K = 1$ MPa$\sqrt{\text{m}}$. As the crack extends into the switched material, the strain mismatch decreases, so that the crack will extend by a finite amount each cycle.

CONCLUDING REMARKS

Various experimental and theoretical aspects of electric field-driven cracking in ferroelectric ceramics are considered in this article. It is demonstrated experimentally that the PLZT ceramic is susceptible to stable crack growth under cyclic electric field with amplitude near or above the coercive field. Pronounced effects of temperature and stress

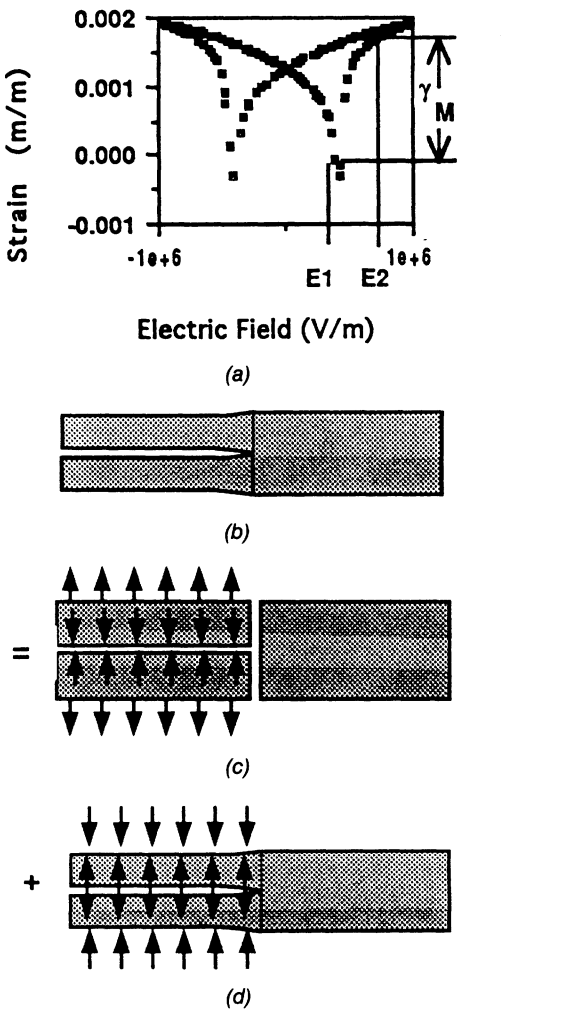

Figure 7. *(a) The strain at two values of electric field; (b), (c), (d) the Eshelby cut-and-paste method gives the strain mismatch.*

on ferroelectric properties are observed, that may affect cracking behavior. Discharge is observed through the gap between two PLZT plates. This observation, if confirmed for the gap between crack faces, would lead to significant modifications to the existing theories of electrostrictive cracks. It is suspected that cracks may extend at both closure and opening. The effects are estimated by mechanics models that rely on mismatch strains induced by electric field near inhomogeneities. Further progress will be made by experimentally ascertaining various factors of the phenomenon, and by performing more rigorous analysis.

ACKNOWLEDGEMENTS

The work was supported by the Office of Naval Research through contracts N00014-93-1-0110 and N00014-93-1-0200. The work of W. Yang was supported by a visiting appointment at the University of California, Santa Barbara funded by ONR through contract N00014-93-1-0110 and by the National Science Foundation of China. The work of Z. Suo was in addition supported by the National Science Foundation through grant MSS-9258115.

REFERENCES

Anstis, G. R., P. Chantikul, B. R. Lawn and D. B. Marshall. "A Critical Evaluation of Indentation Techniques for Measuring Fracture Toughness: I. Direct Measurements", *J. Am. Ceram. Soc.*, 64(9):533–538.

Cao, H. C. and A. G. Evans. 1993. "Non-Linear Deformation of Ferroelectric Ceramics", *J. Am. Ceram. Soc.*, 76(4):890–896.

Cao, H. C., M.-Y. He and A. G. Evans. 1993. "Electric Field-Induced Fatigue Crack Growth in Ferroelectric Ceramics", submitted for publication.

Haertling, G. H. 1987. "PLZT Electrooptic Materials and Applications – A Review", *Ferroelectrics*, 75:25–55.

McMeeking, M. R. 1989. "Electrostrictive Stress near Crack-Like Flaws", *J. Appl. Math. Phys.*, 40:615–627.

McMeeking, M. R. 1990. "A J-Integral for the Analysis of Electrically Induced Mechanical Stress at Cracks in Elastic Dielectrics", *Int. J. Engng. Sci.*, 28:605–613.

Meng, Z. Y., U. Kumar and L. E. Cross. 1985. "Electrostriction in Lead Lanthanum Zirconate-Titanate Ceramics", *J. Am. Ceram. Soc.*, 68:459–462.

Osborn, J. A. 1945. "Demagnetizing Factors of the General Ellipsoid", *Phys. Rew.*, 67:351–357.

Pak, Y. E. 1990. "Crack Extension Force in a Piezoelectric Material", *J. Appl. Mech.*, 57:647–653.

Sosa, H. A. and Y. E. Pak. 1990. "Three-Dimensional Eigenfunction Analysis of a Crack in a Piezoelectric Material", *Int. J. Solids Structures*, 26:1–15.

Suo, Z., C.-M. Kuo, D. M. Barnett and J. R. Willis. 1992. "Fracture Mechanics for Piezoelectric Ceramics", *J. Mech. Phys. Solids*, 40:739–765.

Suo, Z. 1993. "Models for Breakdown-Resistant Dielectric and Ferroelectric Ceramics", *J. Mech. Phys. Solids*, 41:1155–1176.

Tada, H., P. C. Paris and G. R. Irwin. 1985. *The Stress Analysis of Cracks Handbook*. St. Louis, MO: Del Research.

Uchino, K. and A. Furuta. 1992. "Distruction Mechanism of Multilayer Ceramic Actuators", in ONR report on *Materials for Advanced Structural Acoustic Control*, L. E. Cross, ed., Penn State.

Winzer, S. R., N. Shankar and A. P. Ritter. 1989. "Designing Cofired Multilayer Electrostrictive Actuators for Reliability", *J. Am. Ceram. Soc.*, 72:2246–2257.